6 Mass Loss

As was pointed out earlier, mass loss dominates the stellar evolution on the AGB

Nuclear fusion $\sim 10^{-8}\ M_\odot$ yr^{-1}

Mass loss $> 10^{-7}\ M_\odot$ yr^{-1}

Historically it took a long time to appreciate the full magnitude of mass loss on the AGB since the circumstellar material (CSM) only emits appreciably at IR- and short radio-wavelengths, which only became observable in the 1970s. After the data from space infrared observatories such as IRAS (1984) became available, mass loss from AGB stars could be studied systematically.

6.1 Initial-Final Mass Relation

From the point of view of stellar evolution, it is the total, integrated mass loss $\int \dot{M} \mathrm{d}t$ hat is most important. This can be observationally constrained using the ***Initial-Final Mass Relation***, derived from White Dwarf masses in open clusters of known age and distance, see Fig. 20. Due to the paucity of data, this IFMR is not well extremely well established and for example its metallicity dependence is disputed. However, it seems clear that stars with mass 1—6 $M_\odot$ end up as WDs with masses ~ 0.5—1 $M_\odot$.

6.2 Mass loss recipes

To include mass loss in evolutionary calculations requires relating it to the basic stellar parameters. However, as we will see, we lack a detailed understanding of the physical processes behind the mass loss from AGB stars, so mass loss cannot be self-consistently included in evolutionary calculations. However, a number of physical-empirical relations have been suggested, and used in actual calculations. The first of these relations was proposed by Reimers (1975)

$$\dot{M}_{\mathrm{Reimers}} = 4 \times 10^{-13} \eta \frac{(L/L_\odot)(R/R_\odot)}{(M/M_\odot)} \qquad M_\odot \text{ yr}^{-1} \tag{39}$$

where η is a ‘fudge factor’. This relation was really only valid for RGB stars, but since it was simple to use, it also became popular for use on the AGB (but with a higher value for η).

From trying to reproduce the empirical IFMR, Blöcker (1995) proposed a modified form for use during the AGB:

$$\dot{M}_{\mathrm{Bl}} = 4.83 \times 10^{-9} \left(\frac{M}{M_\odot}\right)^{-2.1} \left(\frac{L}{L_\odot}\right)^{2.7} \dot{M}_{\mathrm{Reimers}} \tag{40}$$

Vassiliadis & Wood (1993) proposed another relation, which was derived from fits to observed mass loss rates (see Fig. 21), imposing a maximum mass loss due to a radiation pressure limit (single scattering, see Eq. 55).

$$\dot{M}_{\mathrm{VW}} = \min(\dot{M}_{\mathrm{radpres}}, \dot{M}_{\mathrm{superwind}}) \tag{41}$$

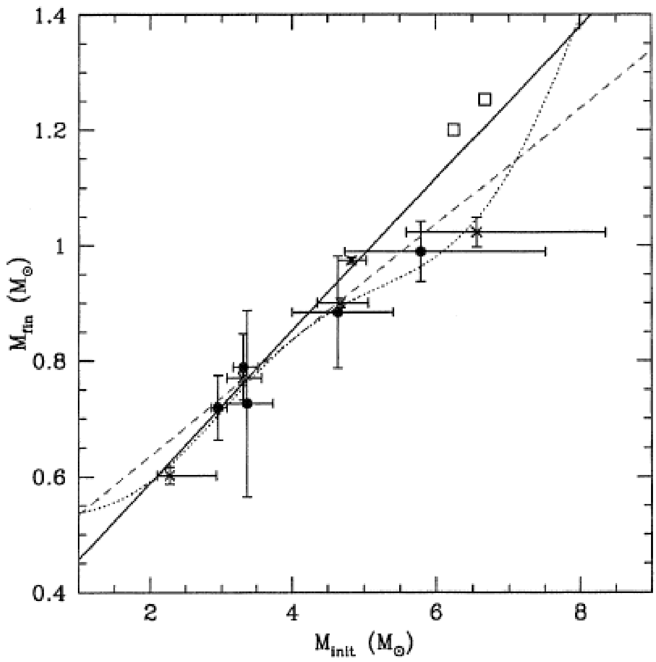

Figure 20: The initial-final mass relation. Filled circles are binned points from open clusters with four or more WDs; crosses are from clusters or binary systems with three or fewer WDs. The solid line is a least-squares linear fit to these points. The dashed line is the linear fit from Ferrario et al. (2005); the dotted line is the inversion of the field WD mass distribution presented in that work. Open squares, which were *not* included in the fits, are from Dobbie et al. (2006) for GD 50 and PG 0136+251. The agreement between these points and the extrapolation of the linear fit is encouraging. From Williams (2006).

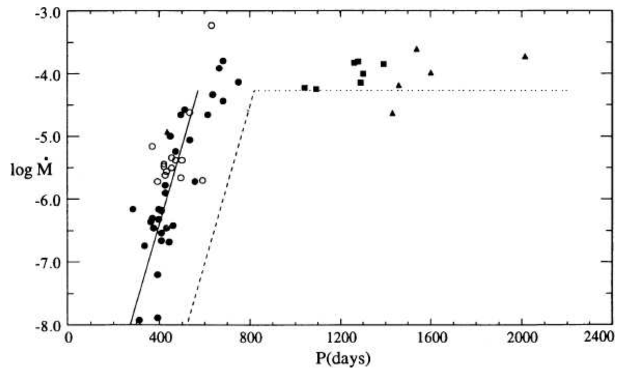

Figure 21: Mass loss rate $\dot{M}$ ($M_\odot$ yr^{-1}) plotted against period for Galactic Mira variables of spectral type M and S (filled circles) and C (open circles) and for pulsating OH/IR stars in the Galaxy (triangles) and the LMC (squares). The solid line is the analytic fit used for low-mass stars ($M < 2.5\ M_\odot$) with the mass loss rates less than the radiation-pressure driven limit. The dashed line is the equivalent relation for a 5 $M_\odot$ star, while the dotted line corresponds to mass loss at the radiation-pressure-driven limit for a typical intermediate mass (5 $M_\odot$) LPV in the LMC with $M_{\rm bol} = -6.5$ and $v_{\rm exp} = 12$ km s^{-1}.

with

$$\dot{M}_{\rm radpres} = \frac{L/c}{v_{\rm exp}}, \qquad \text{with} \quad v_{\rm exp} = -13.5 + 0.056\Pi(\text{days}) \tag{42}$$

$$\log_{10} \dot{M}_{\rm superwind} = -11.4 + 0.0123\Pi(\text{days}) \tag{43}$$

All these are popular recipes, but they lack any profound base in the fundamental physics of the mass loss process.

6.3 Mass loss measurements

The estimated mass loss rates range from 10^{-8} to 10^{-4} $M_\odot$ yr^{-1} (see Fig. 22). The highest values are often referred to as the *super wind*. Typical velocities for the mass loss are in the range 5—30 km s^{-1} (see Fig. 23), so these are relatively slow winds. However, since the temperatures in the winds are also low, they are still supersonic ($c_{\rm s}(100\ {\rm K}) \sim 1$ km s^{-1}).

As we already saw in Fig. 21, there is a relation between mass loss rate and pulsational period. However, this relation is not a simple one, probably because other factors (e.g., metallicity) come in. This is shown more clearly in Fig. 24 which contains a larger sample of AGB stars (separated into M- and C-stars).

Measuring mass loss rates accurately is notoriously difficult. For a steady, spherically symmetric mass loss we have

$$\dot{M} = 4\pi r^2 \rho v\,, \tag{44}$$

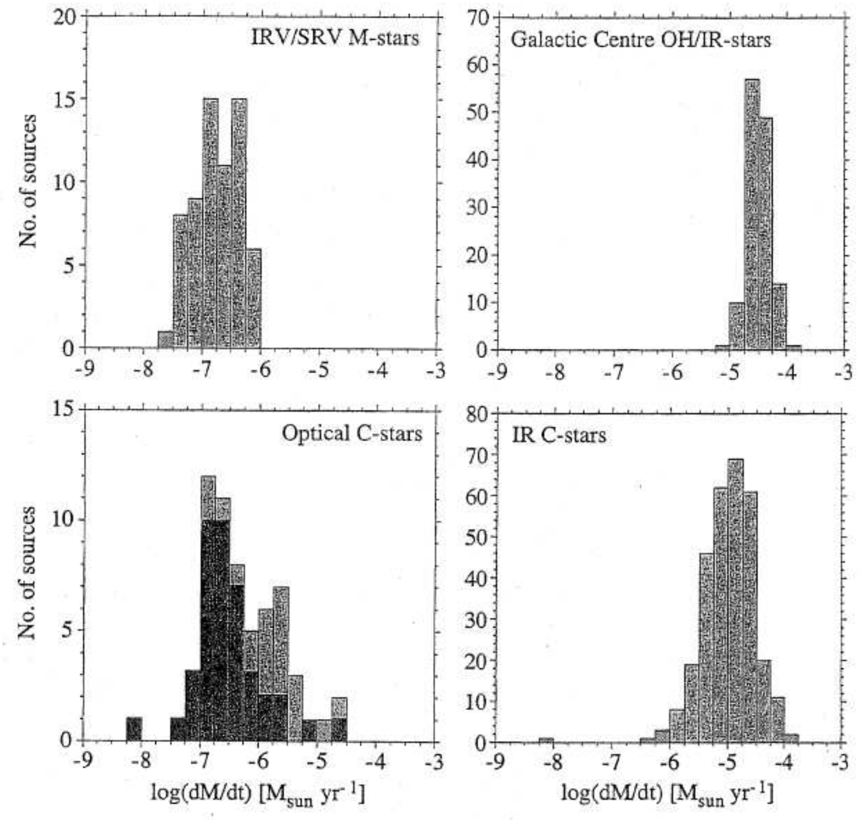

Figure 22: Mass loss rate distributions for two samples of M-stars, and two samples of C-stars. For the optical C-stars, the subsample with stars within about 500 pc is darker. From Olofsson (2004).

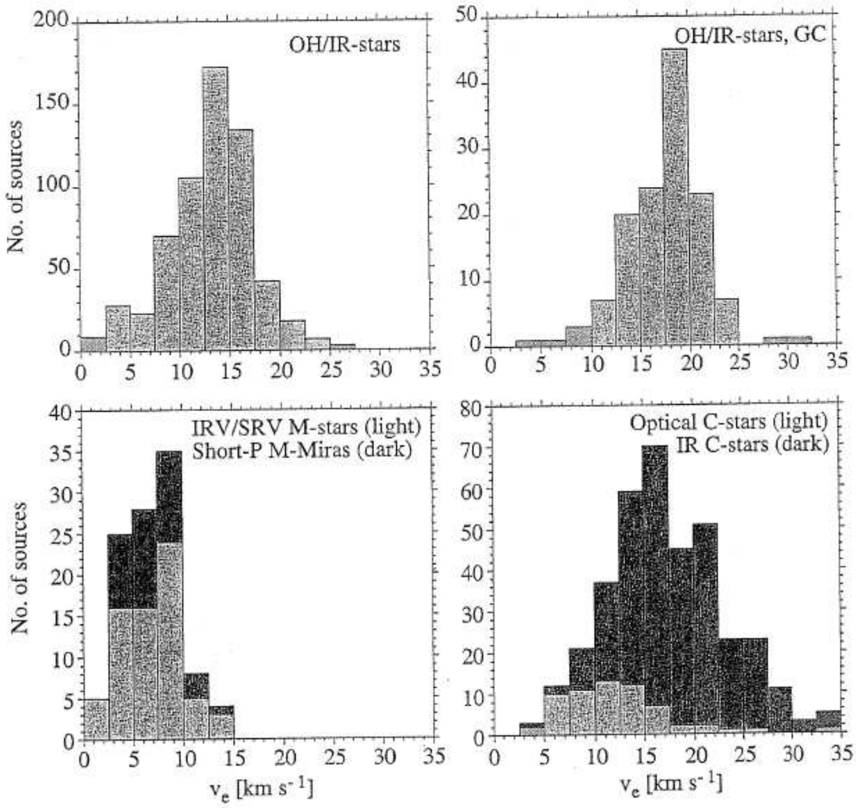

Figure 23: Gas expansion velocity distributions for selected samples of M- and C-stars. From Olofsson (2004).

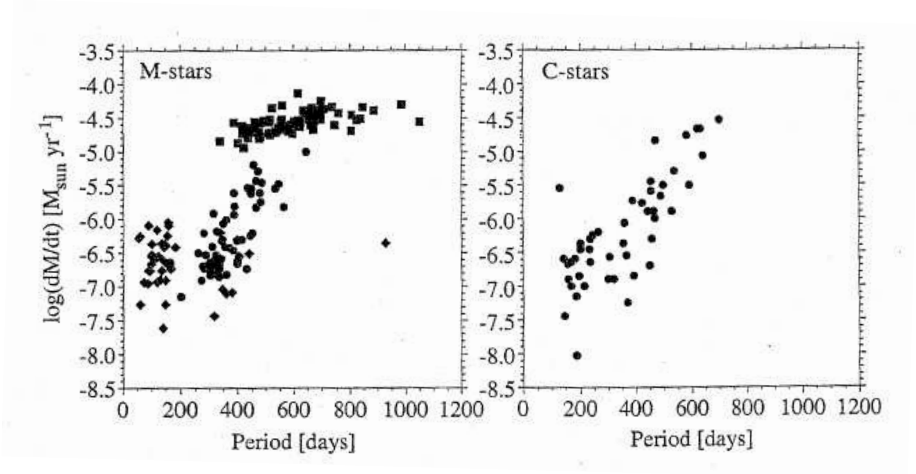

Figure 24: Mass loss rate versus period for three samples of M-stars [SRVs (diamonds), Miras (circles), and Galactic Center OH/IR stars (squares)], and a sample of optically bright C-stars. From Olofsson (2004).

so if the velocity is constant, $\rho \propto r^{-2}$. However, both the mass loss rate and the velocity may vary in time.
To measure $\rho(r)$ we need a 'probe' (atom, molecule, dust grains) emitting radiation. This probe may have a position dependent abundance $A(r)$, depending on the chemistry in the gas. Furthermore, the emissivity of the probe may also vary with radius, depending on the local temperature and radiative transfer effects. So, typically we measure only a small part of the circumstellar medium, and the above effects (abundance, temperature, radiative transfer) are not always easily quantified. Examples of probes for measuring mass loss are: CO thermal emission, dust thermal emission, OH maser emission. We will come back to these later.
A sceptical estimate would be that observed mass loss rates are uncertain with ~ 1 order of magnitude.

6.4 Theory of pulsation/dust-driven mass loss

AGB winds are slow and have high mass loss rates, a combination that has been difficult to achieve with stellar wind models. The observations suggest a connection with the pulsational period (Fig. 24). The only successful models are based on pulsating stellar atmospheres and radiation pressure on dust, see Fig. 28 for a cartoon impression. We will now describe this in some more detail.

6.4.1 Stellar Wind Equation

Stellar winds are radial flows in the star's gravitational field, which means that they need to fulfill certain strict criteria. The momentum equation for the gas can be written

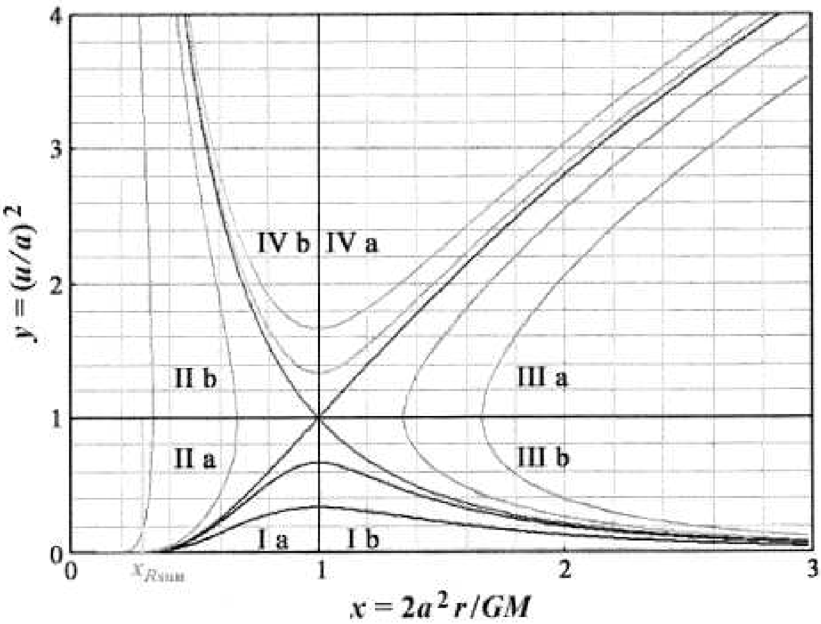

Figure 25: Mathematical solutions for the stellar wind equation. The only solution that represents a stellar wind is the one accelerating through the critical point.

as

$$v\frac{\mathrm{d}v}{\mathrm{d}r} = -\frac{1}{\rho}\frac{\mathrm{d}p}{\mathrm{d}r} - \frac{GM}{r^2} + f(r) \tag{45}$$

(steady flow), where v is the velocity, p is the pressure, ρ the mass density, and $f(r)$ some external force (responsible for driving the mass loss). Combining Eq. 45 with 44 and using the isothermal sound speed $\bar{c}_{\mathrm{s}}^2 = p/\rho$ (different from the adiabatic sound speed $c_{\mathrm{s}}^2 = \gamma p/\rho$), we get

$$\frac{\mathrm{d}v}{\mathrm{d}r} = \frac{v}{v^2 - \bar{c}_{\mathrm{s}}^2}\left(\frac{2\bar{c}_{\mathrm{s}}^2}{r} - \frac{\mathrm{d}\bar{c}_{\mathrm{s}}^2}{\mathrm{d}r} - \frac{GM}{r^2} + f(r)\right) \tag{46}$$

For $v = \bar{c}_{\mathrm{s}}$ this equation has a singularity. In Fig. 25 this point is indicated by (1,1). The lines in that figure represent solutions to Eq. 46. The solution families II and III are multivalued, and therefore unphysical. Stellar wind solutions need to start at low velocity, and keep increasing their velocity until they reach some equilibrium velocity ($v_i nfty$). Figure 25 show that there is only one solution that does, and this is the one that goes through the point (1,1), or $v = \bar{c}_{\mathrm{s}}$, the so-called critical point.
Without an external force $f(r)$ the mass loss is typically weak. This is for example the case for the Sun ($\dot{M}_\odot \sim 10^{-14}\ M_\odot$ yr^{-1}). However, just applying any radial force will not necessarily increase the mass loss rate. The radial dependence of the external force is crucial for its effect on the wind.

First note that for a constant $\bar{c}_{\rm s}$ (i.e. isothermal conditions), the position of the critical point is

$$r_{\rm c} = \frac{GM}{2\bar{c}_{\rm s}^2} - \frac{f(r_{\rm c})r_{\rm c}^2}{2\bar{c}_{\rm s}^2} \tag{47}$$

so if $f(r_{\rm c}) > 0$, $r_{\rm c}$ moves inwards. Since the density is typically higher at smaller radii, the effect is that $\dot{M}$ increases.
However, if $f(r_{\rm c}) = 0$, and $f(r_{\rm c}) > 0$ for $r > r_{\rm c}$, the mass loss will *not* increase. Instead the wind will experience an extra acceleration beyond $r_{\rm c}$ and achieve a higher velocity. The conclusion is thus that high mass loss rates can only be achieved if the extra force operates effectively at or below $r_{\rm c}$.
When the external force is due to continuum radiation it typically has a r^{-2} component, just like gravity. It is therefore useful to write

$$-\frac{GM}{r^2} + f(r) \equiv -(1-\Gamma)\frac{GM}{r^2} \tag{48}$$

and with this definition Eq.47 becomes

$$r_{\rm c}(\Gamma) = \frac{GM(1-\Gamma)}{2\bar{c}_{\rm s}^2} \tag{49}$$

Analysing the wind equation (Eq. 46) we can distinguish three regions

1. $r < r_{\rm c}$: the $\partial p/\partial r$ term dominates and the solution is 'atmosphere-like'.
2. $r \approx r_{\rm c}$: apply the external force in this region to boost the mass loss rate
3. $r > r_{\rm c}$: the $\partial p/\partial r$ term becomes unimportant and the solution is 'wind-like'; apply external force here to boost the wind velocity.

A hydrostatic, stationary atmosphere has an exponential radial density law

$$\rho(r) = \rho_0 \exp\left\{-\frac{r-r_0}{H}\frac{r_0}{r}\right\} \tag{50}$$

$$H = \frac{c_{\rm s}^2}{GM} r_0^2 \tag{51}$$

where H is the so-called scale height and for $r < r_{\rm c}$ the solution to Eq. 46 is indeed very close to this solution.

6.4.2 Scale height problem

For $M = 1M_\odot$, $r_0 = R_* = 300R_\odot$, $T = 2500$ K, we get that $H/R_* = 0.05$, so this means that the density drops rapidly as we move away from the stellar surface. The effect is that even when the force f pushes the critical point $R_{\rm c}$ inward, the mass loss is found to be too low. For example, the parameters $M = 1M_\odot$, $r_0 = R_* = 100R_\odot$, $T = 2500$ K, $\Gamma = 0.5$ give $\dot{M} \sim 10^{-16}\ M_\odot$ yr^{-1}.
However, for a pulsating atomosphere, the effective scale height will be substantially larger. The reason is that the pulsations create sound waves which travel outward,

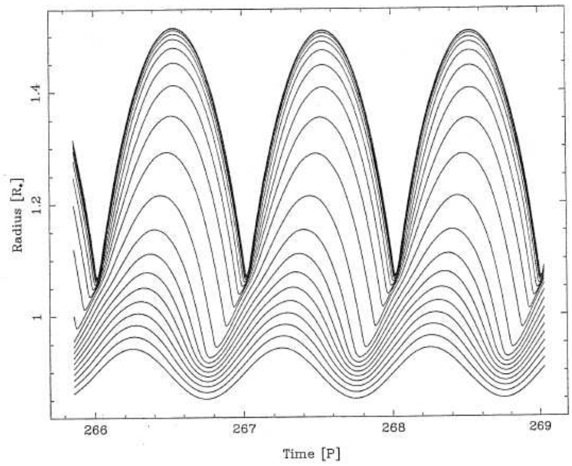

Figure 26: Position of selected mass shells as a function of time for a dynamical model atmosphere (Höfner et al. 2003) with the following parameters: $T\text{eff} = 2800$ K, $L = 7000\ L_{\odot}$, $M = 1\ M_{\odot}$, $\epsilon_{\rm C}/\epsilon_{\rm O}$, $\Pi = 390$ days, and piston velocity amplitude 2 km s^{-1} (Time in periods, radius in units of the photospheric radius $R_* = 355\ R_{\odot}$ of the hydrostatic initial model.

effectively 'lifting up' the atmosphere. In fact the sound waves will often steepen into shock waves, causing substantial compression, thus increasing the density even more. A simple energetic argument can be used to estimate the magnitude of this effect.
If a shell of mass $M_{\rm s}$ is accelerated by a shock of velocity v_0, it will acquire a kinetic energy $\frac{1}{2}M_{\rm s}v_0^2$. This will allow it to travel to a radius $r_{\rm max}$ given by

$$\frac{1}{2}M_{\rm s}v_0^2 = -GMM_{\rm s}\left(\frac{1}{r_{\rm max}} - \frac{1}{r_0}\right) \qquad \Rightarrow \tag{52}$$

$$\frac{r_{\rm max}}{r_0} = \left(1 - \left(\frac{v_0}{v_{\rm esc}}\right)^2\right)^{-1} \tag{53}$$

For $M = 1M_{\odot}$, $r_0 = R_* = 300R_{\odot}$, we get $v_{\rm esc} = 35$ km s^{-1}. If we take $v_0 = 15$ km s^{-1} (from observations), we get that $r_{\rm max}/r_0 \approx 1.3$, so the shock waves will lift the atmosphere by a substantial factor. Detailed numerical hydrodynamic models give roughly the same number (see Fig. 26).
In fact, the increased time-averaged scale height of such a pulsating atomosphere (see Fig. 27) can become so high that this process alone can set up a mass outflow. However, also this wind has too low a mass loss rate to explain the winds from AGB stars.

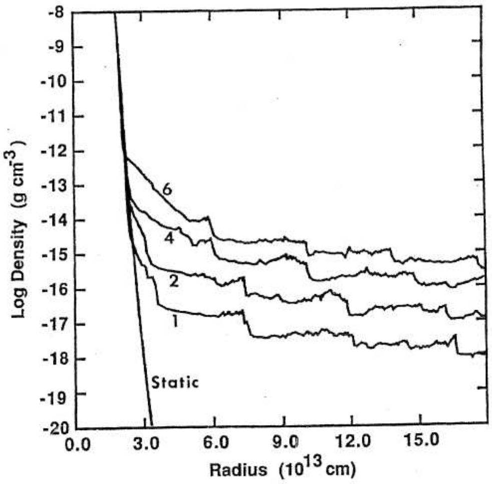

Figure 27: The density versus r as influences by shocks in a Mira variable. The density falls roughly as r^{-5} just above the hydrostatic region and falls roughly as r^{-3} in the outermost region. The curves are labeled with the velocity amplitude (in km s^{-1}) of the pulsations. Notice that the scale of the density for the region beyond the static base is set by the amplitude of the pulsation, Δv. From Bowen (1988).

6.4.3 Radiation pressure

The force thought to be responsible for driving the high mass loss rate winds from AGB stars is radiation pressure on dust. For the the process the Γ factor can be written as

$$\Gamma_{\rm d} = \frac{\kappa_{\rm rp} L_*}{4\pi c G M} \tag{54}$$

where $\kappa_{\rm rp}$ is the mean opacity for radiation pressure. This $\kappa_{\rm rp}$ is much higher for dust particles than for gas particles, making them a particularly efficient agent for accelerating the gas.

Let us look at what mass loss we can get from radiation pressure. Each photon carries a momentum $h\nu/c$. If it transfers this to *one* dust particle one can obtain an estimate for the mass loss rate. The total momentum rate in the photons is L_*/c, and the total momentum rate in the wind is $\dot{M} v_\infty$, implying that

$$\dot{M} = L_*/(c v_\infty)\,, \tag{55}$$

an estimate that is known as the *single scattering limit*. For $L_* = 10^4\ L_\odot$, $v_\infty = 10$ km s^{-1}, we get from this limit $\dot{M} = 2 \times 10^{-5}\ M_\odot$ yr^{-1}, a very appreciable mass loss rate for an AGB star. We saw above that the mass loss recipe of Vassiliadis & Wood (1993) was using this limit.

However, the single scattering limit is a very conservative estimate. Note that if one considers the energy budget instead of the momentum one, the energy rate in the wind is $L_{\rm wind} = \frac{1}{2}\dot{M}v_\infty^2$, which is much less than the available energy rate in the photons L_*, since in the single scattering limit $L_{\rm wind}/L_* = \frac{1}{2}v_\infty/c \ll 1$. This suggests that a higher mass loss should be possible. This can be achieved through *multiple scatterings*. If we take the wind momentum equation Eq. 45 and integrate it over $\mathrm{d}m = 4\pi r^2 \mathrm{d}r$ from the stellar photosphere to infinity, we get

$$\int_{R_*}^{\infty} 4\pi r^2 \rho v \frac{\mathrm{d}v}{\mathrm{d}r}\mathrm{d}r + \int_{R_*}^{r_c} \left[\frac{1}{\rho}\frac{\mathrm{d}p}{\mathrm{d}r} + \frac{GM}{r^2}\right]\mathrm{d}m$$
$$+ \int_{r_c}^{\infty} \frac{1}{\rho}\frac{\mathrm{d}p}{\mathrm{d}r}\mathrm{d}m + \int_{r_c}^{\infty} \frac{GM}{r^2}(1-\Gamma_{\rm d})\rho 4\pi r^2 \mathrm{d}r = 0 \tag{56}$$

The first integral is actually the momentum rate in the wind $\dot{M}v_\infty$, since the velocity at R_* will be much less than v_∞. The second integral considers the pressure and gravity force below the critical point. Since the flow is close to hydrostatic equilibrium in that region, this term can be taken zero. The third integral does not contribute much as the gas pressure gradient is no longer important beyond the critical point (in the supersonic part of the wind). We thus get from Eq. 56

$$\dot{M}v_\infty = 4\pi G M_* (\Gamma_{\rm d} - 1)\int_{r_c}^{\infty} \rho \mathrm{d}r \tag{57}$$

but since the optical depth in the wind is defined as

$$\tau_{\rm w} = \int_{r_c}^{\infty} \kappa_{\rm rp}\rho \mathrm{d}r \tag{58}$$

we find that

$$\dot{M}v_\infty = \frac{L_*}{c}\left(\frac{\Gamma_{\rm d}-1}{\Gamma_{\rm d}}\right)\tau_{\rm w} \approx \frac{L_*}{c}\tau_{\rm w} \quad \text{for} \quad \Gamma_{\rm d} \gg 1 \tag{59}$$

where we have used Eq. 54.
So for a high optical depth, $\dot{M}$ can be substantially higher than the single scattering value. However, the value for $\tau_{\rm w}$ cannot be arbitrarily high. We already saw that we get an absolute maximum due to the available energy. This gives

$$\tau_{\rm w} < \frac{2c}{v_\infty} \tag{60}$$

Taking into account the fact that stellar luminosity is reduced due to its use as wind accelerator, one in fact find a more strict

$$\tau_{\rm w} < \frac{c}{v_\infty} = 27\sqrt{\frac{\dot{M}/10^{-5}}{L/10^5}} \tag{61}$$

6.4.4 Velocity distribution

To find the velocity at infinity we can use the momentum equation beyond r_c where the pressure terms can be neglected

$$v\frac{\mathrm{d}v}{\mathrm{d}r} = \frac{1}{2}\frac{\mathrm{d}v^2}{\mathrm{d}r} = \frac{GM}{r^2}(\Gamma_{\rm d} - 1) \tag{62}$$

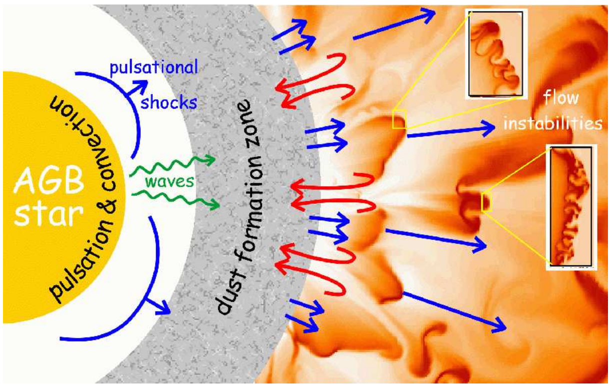

Figure 28: A cartoon-like representation of the wind forming region around an AGB star. From Woitke.

Integrating this from $r_{\rm c}$ until ∞ gives

$$v^2(r) = v^2_(r_{\rm c}) + v^2_\infty \left(1 - \frac{r_{\rm c}}{r}\right) \tag{63}$$

$$v^2_\infty \equiv \frac{2GM_*}{r_{\rm c}}(\Gamma_{\rm d} - 1) = v_{\rm esc}\frac{R_*}{r_{\rm c}}(\Gamma_{\rm d} - 1) \tag{64}$$

The last expression shows that v_∞ is typically of order the escape velocity from the stellar surface (since $\Gamma > 1$ and $r_{\rm c} > R_*$). If we substitute $M = 1M_\odot$, $L_* = 10^4\ L_\odot$, $r_{\rm c} = 2 \times 10^{14}$ cm, we get $v_\infty = 16$ km s^{-1} and at $r = 5r_{\rm c}$ already 90% of this value has been reached.

6.5 The role of dust

For a complete picture of the mass loss process we need two more ingredients

- dust formation
- gas-dust coupling

6.5.1 Dust formation

Dust formation is a complicated issue, of which we have only limited understanding. Observationally it is clear that AGB stars form two different types of dust grains

Carbon stars amorphous carbon grains

M-type stars ‘dirty’ silicates

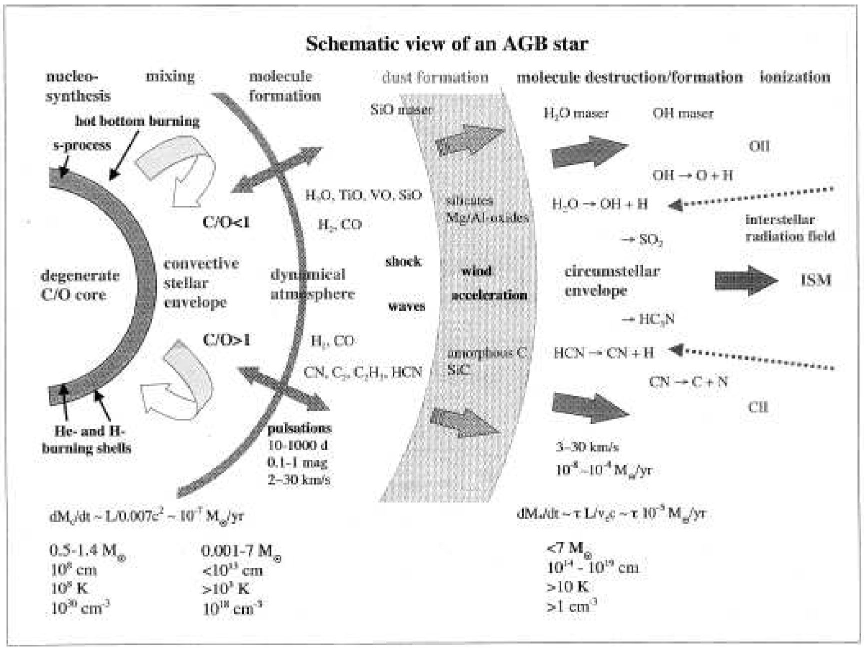

Figure 29: As Fig. 28, but with detailed labelling of the various regions and the relevant physical processes, and showing the differences between O- and C-rich stars. From Hron.

Although the silicates are more common, we have a better understanding of carbon grain formation (partly due to research carried out for non-astrophysical reasons). Carbon as an element can easily form long chain-like molecules, and from those chains rings (so-called Polyaromatic Hydrocarbons, PAHs) and sheets may form. These may then aggregate into amorphous carbon grains.
To handle this complex chemistry in simulations, a statistical description was developed, known as *nucleation theory*. It starts by considering a distribution function $f(N)$ of so-called monomers (C atoms in the case of carbon dust), where for example f(4) would be the fraction of carbon aggregates containg 4 C atoms. By introducing terms for growth ('sticking') and diminshment (evaporation, 'sputtering') this distribution function can be evolved in time. Matters are further simplified by using integrated moments of this distribution, for example the term

$$K_2 = \sum_{N_l}^{\infty} f(N) N^{2/3} \tag{65}$$

is proportional to the total surface area of the grain population.
Dynamical models including grain formation (using nucleation theory) show are able to produce typical AGB winds, suggesting that we largely understand the mass loss physics in C-stars, at least for the simplified case of a steady, spherical wind.

6.5.2 Dust-gas coupling

The radiation pressure works only on the dust particles, which only form a small fraction of the material. So in order to set up a wind, the motion of the dust has to be transferred to the gas particles. This happens via collisions. The collective effect of the gas on the dust is known as the 'drag', and can be expressed as a force, which can be approximated as

$$f_{\rm drag} = \sigma_{\rm d} n_{\rm g} n_{\rm d} m_{\rm g} |v_{\rm coll}| v_{\rm drag} \tag{66}$$

$$\text{with} \qquad v_{\rm drag} \equiv |v_{\rm g} - v_{\rm d}| \tag{67}$$

$$\text{and} \qquad v_{\rm coll} = v_{\rm thermal} \sqrt{\frac{64}{9\pi} + \left(\frac{v_{\rm drag}}{v_{\rm thermal}}\right)^2} \tag{68}$$

where $\sigma_{\rm d}$ and $m_{\rm g}$ are the dust cross section and the gas particle mass , $n_{\rm g}$ and $n_{\rm d}$ are the gas and dust number densities, $v_{\rm coll}$ is the collision velocity, and $v_{\rm thermal}$ the typical thermal velocity of the gas (as obtained from the Maxwell-Boltzmann distribution). The drag force tries to minimize the drag velocity $v_{\rm drag}$, but is also proportional to $v_{\rm drag}$. This means that there will be an equilibrium value for $v_{\rm drag}$. Usual approximations assume either $v_{\rm drag} = 0$ ('perfect coupling') or $v_{\rm drag} = v_{\rm drag}^{\rm eq}$ ('momentum coupling').

6.5.3 Dust formation in O-rich AGB stars

The dust around M-type stars is Si-based. Si behaves chemically different from C, it does not form large chains and sheets. Therefore these dust particles cannot grow

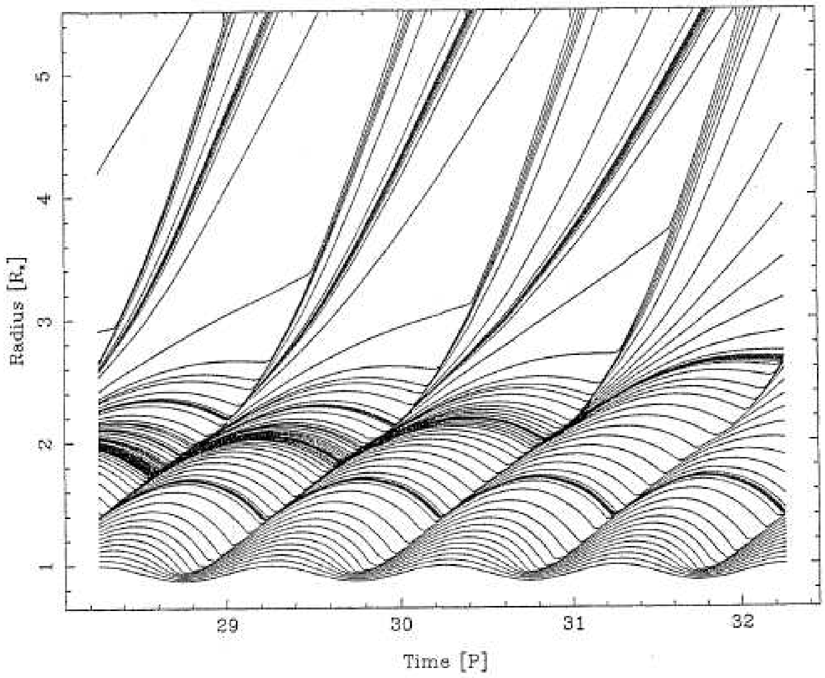

Figure 30: Positions of selected mass shells as a function of time for a model of a carbon dust driven wind (Höfner & Dorfi 1997). During each new pulsation cycle a new dust layer is formed, triggered by enhanced density behind the shock waves. Below about 2 R_* the dustfree atmosphere is periodically passed by strong shocks (marked by sharp bends in the lines). The formation of dust layers and their subsequent acceleration due to radiation pressure (indicated by the steepening of the lines) takes place between 2 and 3 R_*. Time in pulsation periods, radius in units of the stellar radius R_* of the corresponding hydrostatic initial model.

gradually, but rather have to condense out from the gas phase into the solid phase. This happens when the partial pressure is larger than the vapor pressure: $P_{\rm p} > P_{\rm v}$, where $P_{\rm p} = n_{\rm molecule} k_{\rm B} T$ and $P_{\rm V} = P_{\rm M} \exp(-T_{\rm M}/T)$. $P_{\rm M}$ and $T_{\rm M}$ are properties of the molecule under consideration.

The silicon oxides SiO and SiO_2 do not condense out at high temperatures, but other molecules like TiO, TiO_2, Al_2O_3 (corundum) do. It is therefore thought that these form the seed nuclei for Si-grain growth. The full grown silicate grains are made 'dirty' by both Mg and Fe silicates. The dirt is necessary for these grains to absorb radiation from the star, as pure silicates would be too glassy and transparent. Still, detailed modelling of winds driven by silicate grains show that it is difficult to condense enough dirty silicates around the critical point, which is where they are needed in order to produce a high mass loss wind. We have therefore currently no working model for explaining the mass loss from M-type AGB stars.